Hearing Research 371 (2019) 40–52

Contents lists available at ScienceDirect

Hearing Research

journal homepage: www.elsevier.com/locate/heares

Research Paper

Intracochlear near infrared stimulation: Feasibility of optoacoustic stimulation *in vivo*

Peter Baumhoff [a, *], Nicole Kallweit [b, c], Andrej Kral [a, c]

[a] Institute of AudioNeuroTechnology and Department of Experimental Otology, ENT Clinics, Hannover Medical School, Stadtfelddamm 34, 30625, Hannover, Germany
[b] Laser Zentrum Hannover e.V. (LZH), Hollerithallee 8, 30419, Hannover, Germany
[c] DFG Cluster of Excellence, Hearing 4 All, Germany

ARTICLE INFO

Article history:
Received 4 July 2018
Received in revised form
4 October 2018
Accepted 8 November 2018
Available online 12 November 2018

Keywords:
Near infrared stimulation
Laser
Optoacoustic effect
Cochlea
Inferior colliculus
Guinea pig

ABSTRACT

Intracochlear optical stimulation has been suggested as an alternative approach to hearing prosthetics in recent years. This study investigated the properties of a near infrared laser (NIR) induced optoacoustic effect. Pressure recordings were performed at the external meatus of anaesthetized guinea pigs during intracochlear NIR stimulation. The sound pressure and power spectra were determined. The results were compared to multi unit responses in the inferior colliculus (IC). Additionally, the responses to NIR stimulation were compared to IC responses induced by intracochlear electric stimulation at the same cochlear position to investigate a potentially confounding contribution of direct neural NIR stimulation. The power spectra of the sound recorded at the external meatus ($n = 7$) had most power at frequencies below 10 kHz and showed little variation for different stimulation sites. The mean spike rates of IC units responding to intracochlear NIR stimulation ($n = 222$) of 17 animals were significantly correlated with the power of the externally recorded signal at frequencies corresponding to the best frequencies of the IC units. The response strength as well as the sound pressure at the external meatus depended on the pulse peak power of the optical stimulus. The sound pressure recorded at the external meatus reached levels above 70 dB SPL peak equivalent. In hearing animals a cochlear activation apical to the location of the fiber was found. The absence of any NIR responses after pharmacologically deafening and the comparison to electric stimulation at the NIR stimulation site revealed no indication of a confounding direct neural NIR stimulation. Intracochlear optoacoustic stimulation might become useful in combined electro-acoustic stimulation devices in the future.

1. Introduction

Pulsed laser irradiation has been discussed as an alternative for stimulation of peripheral nerves (Tozburun et al., 2012; Duke et al., 2009; Wells et al., 2007a) since it avoids the disadvantage of a spreading electric field. Pulsed lasers in the near infrared range (NIR) have therefore been fathomed within auditory research (Tian et al., 2017; Guan et al., 2016; Tan et al., 2015; Richter et al., 2011a; Rajguru et al., 2010). NIR pulses were, however, shown to activate hair cells (Richardson et al., 2017; Thompson et al., 2015; Rettenmaier et al., 2014; Schultz et al., 2014; Verma et al., 2014; Teudt et al., 2011). In those *in vivo* studies that involved profound hearing loss, compound action potentials (CAPs) could not be evoked during intracochlear laser stimulation (Thompson et al., 2015; Schultz et al., 2012, 2014), contradicting the possibility to stimulate spiral ganglion cells (SGN) directly. Absorption of pulsed lasers in water generate pressure waves that are acoustically well within hearing range, considering both frequency content and sound pressure levels (Kallweit et al., 2016; Xia et al., 2016; Schultz et al., 2012, 2014; Teudt et al., 2011).

Such optoacoustic effects could under certain conditions be beneficial, particularly for subjects with residual hearing. The optoacoustic signal could be used in combined opto-electric hearing devices for electro-(opto)acoustic stimulation and could be advantageous due to the exceptionally small size of the sound-delivering object (the stimulating glass fiber) that can be easily placed even into the scala tympani. The inclusion of either an

* Corresponding author. Institute of AudioNeuroTechnology, Stadtfelddamm 34, 30625, Hannover, Germany.
E-mail addresses: baumhoff.peter@mh-hannover.de (P. Baumhoff), nicolekallweit@gmx.de (N. Kallweit), kral.andrej@mh-hannover.de (A. Kral).

https://doi.org/10.1016/j.heares.2018.11.003

optical fiber or a laser diode into an integrated CI design could be used to apply optoacoustic intracochlear pressure, analogous to an actuator, and confer low frequency envelope information to hair cells apically to the electrically stimulated (high frequency) regions. Pilot tests of the efficiency of envelope coding with stimuli corresponding to intracochlear optoacoustic signals showed promising results, particularly when considering the high-frequency hearing loss in EAS subjects (Krüger et al., 2017). The instantaneous optical output could be synchronized with the electric stimulation more easily than the delayed acoustic input from hearing aids, as used in current techniques. However, many possible drawbacks need to be also considered.

In the present study, the optoacoustic phenomena were characterized *in vivo* to explore the possibility of an application in hearing impaired subjects with residual low frequency hearing. In order to evaluate the feasibility of such an approach, we determined whether the optoacoustic activation of the cochlea is strong enough in medium to low frequencies to evoke above threshold responses. To access the feasibility of optoacoustic stimulation direct neural stimulation has to be excluded as confounding stimulation mode. We combined *in vivo* intracochlear optical stimulation with neuronal recordings along the tonotopic axis of the inferior colliculus (IC) in the auditory midbrain of normal hearing animals and pressure recordings through a condenser microphone at the external ear canal. We verified the optoacoustic origin of the IC activation by absence of responses to optical stimuli in deafened animals and comparison to electrical stimulation. Furthermore, we assessed the pressure spread in the cochlea by computing the power spectrum of sound at the external ear and compared it to the tonotopic frequency range activated in the IC. Finally, we did not find any signs of confounding direct neuronal stimulation by pulsed laser in the present experiments.

2. Materials and methods

All experiments of the present study were performed in 23 (5 female) adult, normal hearing Dunkin-Hartley (albino) guinea pigs (485.2 g ± 130.7 g). All animals were handled and housed according to German (TierSchG, BGBl. I S. 1206, 1313) and European Union (ETS 123; Directive 2010/63/EU) guidelines for animal research and the described animal experiments were approved by German state authorities (Lower Saxony State Office for Consumer Protection and Food Safety [LAVES] approval number 14/1514) and monitored by the institute's animal welfare officer.

2.1. Surgical preparation

Anesthesia was induced by an intramuscular injection of a combination of ketamine (50 mg/kg), xylazine (10 mg/kg) and atropine sulfate (0.1 mg/kg). During the surgery and throughout the experiments vital parameters and anesthesia level were continuously assessed by monitoring heart rate (ECG) and capnometry (CO_2%/vol.). The absence of paw-withdrawal and corneal reflexes was tested in regular intervals. Appropriate anesthesia level was maintained by follow-up injections of 20%–30% of the initial dose of ketamine and xylazine in intervals of 45 min or as needed. In some cases, the xylazine dosage was reduced by half for cardiac relief after all surgical procedures were completed. During the experiments, the body temperature was measured via a rectal probe and the maintained between 37.5 and 38.5 °C using a heating blanket (TC-1000 Temperature Controller, CWE Inc., Ardmore, USA). A custom-made endotracheal tube was inserted through a tracheotomy and was connected to a capnometer (Normocap CO_2 & O_2 Monitor, Datex, Helsinki, Finland). The animals were either breathing spontaneously or, if required, were artificially ventilated (Rodent Ventilator 7025, Ugo Basile, Comerio, Italy).

To fit a skull mounted head holder, the animal's head was positioned in a stereotactic frame (Stereotaxic Frame 1430, David Kopf Instruments, Tujunga, USA) and initially fixed by ear bars (Non-Rupture Ear Bars 855, David Kopf Instruments) and a custom built snout holder. The skull was exposed dorsally and a purpose build, stainless steel fixation-rod was cemented onto the ossa nasales, anterior to suture-point Bregma using dental-acrylic (Paladur, Heraeus Kulzer GmbH, Dormagen, Germany) and 3 to 4 bone screws (Ø 0.85 mm, Fine Science Tools GmbH, Heidelberg, Germany). A hole was drilled near Bregma to place a reference silver ball electrode onto the Dura mater. Stable electric contact of the reference was established using salt-free electrode gel (Spectra 360, Parker Laboratories, INC., Fairfield, USA), which was filled into the trepanation hole. After complete polymerization of the dental acrylic, the ear bars as well as the snout holder were removed.

Both tympanic bullae were opened after retro-auricular incision and retraction of the skin. At each side a cochleostomy was drilled into the basal cochlear turn approximately 0.6 mm below the round window. The pre- and post-surgical hearing status was verified by ABR recordings (see acoustic stimulation for details). One cochlea (ipsilateral to the later recording site) was deafened (deafening procedure see below) to eliminate acoustic crosstalk between the cochleae by bone- or air-conduction.

The skull was opened contra-lateral to the stimulation side, centered 12 mm caudally from Bregma and 4 mm laterally from the midline and the *Dura mater*. The opening had an approximate diameter of 7 mm. The stereotactic frame and the animal's head were positioned in a way that allowed access to the ipsi-lateral cochleostomy. A linear single-shank electrode array with 16 iridium contacts spaced by 100 µm and an site area of 177 μm^2 (NeuroNexus, Ann Arbor, USA) or a 32 channel double shank array with the described specifications for both shanks (ditto) was stereotactically inserted into the Inferior colliculus (IC) through the overlaying cerebral cortex. The insertion site was in the middle of the trepanned area and the latero-medial insertion angle was set to ~35–45° relative to midline. Prior to the recordings the brain was covered with medical grade silicon oil (M 5000, Carl Roth GmbH & Co. KG, Karlsruhe, Germany) to prevent dehydration of the brain tissue.

The position of the recording track was histologically verified after the experiment. To verify the stereotactic electrode position at the beginning of the study, the electrode array was stained with a fluorescent cell labeling solution (DiI or DiO, Life Technologies, Carlsbad, USA) prior to insertion in some cases for a better visibility of the electrode track (Fig. 1 A).

2.2. Acoustic stimulation

The hearing thresholds were tested prior to surgery, after cochleostomy and after deafening, by recording ABRs evoked by 50 µs clicks at increasing sound pressure levels (0–80 dB peSPL, 5 dB steps). The stimuli were typically presented with 100 repetitions through a headphone speaker (DT48, Beyerdynamic, Heilbronn, Germany). The signals were amplified by 100 dB and filtered between 200 Hz and 5 kHz (6th order butterworth filter). Normal hearing was presumed for threshold-levels of 35 dB peSPL or below. All animals had normal hearing after insertion of the electrode array into the midbrain. The intra-collicular position was verified by measuring frequency response curves (Fig. 1 B). We stimulated with 50 ms tone bursts (5 ms cosine ramp) at frequencies between 1 and 32 kHz with 4 steps per octave for sound pressure levels from 0 to 90 dB SPL_{rms} in 10 dB steps through the headphone speaker positioned ~ 3 cm from the ear, contralateral to the recording site. Stimulation and recordings were operated

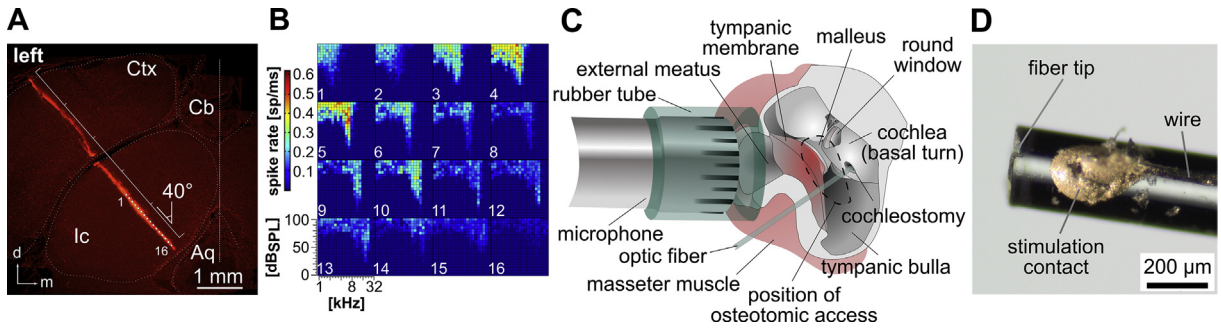

Fig. 1. Inferior colliculus (IC) recordings and optical stimulation approach. **A**, Example of the histological verification of the electrode position in the IC. For a histologic verification of the penetration path and the electrode position in the IC, the recording electrode array was stained with the fluorescent dye DiI prior to insertion. In the example shown, the electrode was inserted in a 40° angle to position the 16 electrodes through the central part of the IC (Aq: cerebral aquaeduct; Ctx: cortex; Cb; cerebellum; Ic: inferior colliculus; d: dorsal; m: medial). **B**, Exemplary frequency response areas in the IC. For the verification of the IC position during the experiments, we recorded the neuronal frequency response areas. Mean spike rate during 50 ms pure tone stimulation is plotted as a function of stimulation frequency and sound level for the 16 intra-collicular recording positions marked in A. The characteristic frequency (CF) at the tip of each frequency response area gradually increases from low frequencies at the more superficial to high frequencies at the deeper contacts, indicating an electrode penetration along the tonotopic axis of the central IC. **C**, Schematic representation of the setting for stimulation and pressure recording. We stimulated optically by a cochleostomic insertion of an optical fiber into the scala tympani in the basal cochlear turn. The intracochlear position could be varied by changing insertion angle and depth of the fiber. We recorded the pressure at the external meatus by positioning a condenser microphone over the cartilageous external ear canal and loosely sealing it with a fitted rubber ring. **D**, Photograph of the end of the optical fiber. Close to the light emitting fiber tip a stimulation contact was placed with conductive varnish. It was connected to a 1 pin gold connector (not shown) by an insulated platinum micro wire. The custom design was prepared by MedEl Comp., Innsbruck, Austria. (For interpretation of the references to color in this figure legend, the reader is referred to the Web version of this article.)

through a custom recording setup and software (AudiologyLab, Otoconsult, Franfurt a.M., Germany). The stimulation level was calibrated through the software at each frequency prior to each recording using a condenser microphone (1/4" microphone [4939] in combination with a preamplifier [2670] and a Nexus conditioning amplifier [2690], Brüel & Kjaer, Nærum, Denmark) perpendicular to the sound path between ear and speaker. The stimuli were presented in randomized order with 10 repetitions for each stimulus. The neuronal signals were acquired and amplified through a multichannel recording system (Lynx-8 amplifier system, amplification 5000–10000 times, butterworth filter 1 Hz - 9 kHz, rolloff: 12 dB per octave, Neuralynx, Bozeman, USA) and stored through AudiologyLab at a sampling rate of 25 kHz using a 32-channel MIO card (NI-6259 National Instruments, Austin, USA). Directly after the recording, we verified the electrode placement by determining the characteristic frequencies (CFs) of the multi unit responses at the electrode contacts of the array using custom-made Matlab routines (MathWorks, Natick, MA, USA). Throughout the manuscript each multi unit response is referred to as 'unit'. We assumed the position to be intra-collicular, when CFs progressively increased from superficial to deep recordings (Fig. 1 B). For later analysis, the cumulative best frequency (cBF) was defined as the frequency with the highest summed response rate over all stimulation levels. This cBF is closely correlated with the CF as shown previously (Konerding et al., 2018) with a tendency of being slightly lower than the CF. We chose this measure, to account for the uncertainty of the intensity level of the optoacoustic stimulation, which, considering the response strength, in many cases seemed to be well above threshold.

2.3. Optical stimulation

Two different laser systems were employed for optical stimulation. A tunable laser-system, based on an optical parametric oscillator (OPO, Ekspla, NT342A, Vilnius, Lithuania), produced 5 ns pulses at a repetition rate of 10 Hz. Wavelengths were tunable between 420 and 2300 nm. The energy output of this system was calibrated prior to the experiment using a pyroelectric energy probe (DPJ8, Spectrum Detector Inc., Oregon, USA). A second laser system generated adjustable pulse durations between 10 µs and 20 ms in a wavelength range between 1848 and 1862 nm (Capella R-1850, Lockheed Martin Aculight, Bothell, USA). This system's energy output was calibrated using a thermopile sensor (P10Q, Coherent Inc., Portland, USA) coupled to a power and energy meter (LabMax-TOP, Coherent Inc., Portland, USA).

After the position of the electrode-array within the IC had been confirmed, a cleaved optical multimode-fiber (low OH, core diameter either 105 µm [FG 105LCA] or 200 µm [FG 200LCC], Thorlabs, Newton, USA) was inserted into the basal turn through the cochleostomy. The fiber was coupled to either laser system by a SMA connector. The insertion was directed by a micro manipulator (MM33, Märzhäuser Wetzlar GmbH & Co. KG, Wetzlar, Germany) and the fiber-tip was either pointed towards the basilar membrane or towards the osseous spiral lamina.

The parameters of the optical stimuli used in this study are summarized in Table 1. For stimulation at different wavelengths and pulse durations in the ns and µs range the energy output was often set to 6 µJ, a pulse energy that elicited robust CAP responses and measurable sound pressures in earlier studies (Kallweit et al., 2016; Schultz et al., 2012). The responses to these stimuli were recorded in the IC. After successful stimulation in the normal hearing ear, this ear was also deafened (deafening procedure see below). Then laser-stimulation was repeated and IC responses were measured. Afterwards electric stimulation followed (see below).

In 6 cases both laser systems were used for stimulation in the same preparation. In these cases the optical stimulations were performed sequentially. Each system was connected to a separate optical fiber, in order to individually calibrate the output energy

Table 1
Summary of the optical stimulation parameters used in the study.

laser system	wavelength	pulse energy	pulse peak power	pulse duration
Capella	1850 nm/1860 nm	≤3 mJ	≤150 mW	10 µs to 20 ms
Ekspla	420 nm–2300 nm	1 µJ–15 µJ	~2 kW	5 ns

prior to the *in vivo* experiments. Therefore the fiber of the first system was retracted from the cochleostomy and the fiber of the second system was inserted. We used a micromanipulator to keep the insertion depth and angle constant for stimulation with both systems.

2.4. Electric stimulation

In 10 ears (N = 7 animals), customized 200 μm optical fibers ([FG 200LCC], Thorlabs, Newton, USA) with a conductive contact at the fiber-tip (Fig. 1D; MedEL, Innsbruck, Austria) were used for optical stimulation with the Capella laser system. This special design enabled an additional monopolar electric stimulation in close proximity to the site of light emission and absorption. Biphasic charge balanced electric pulses with a phase-duration of 100 μs were generated by a custom stimulation system (Otoconsult, Frankfurt a.M., Germany). Varying current levels between 30 μA and 1 mA, in 1 dB steps were used for electric stimulation. Responses to electric stimulation were analyzed 1 dB above threshold, if not indicated otherwise.

2.5. Deafening procedure

The animals were deafened by slowly applying 2.5–5% neomycin-sulfate (Caesar & Lorentz GmbH, Hilden, Germany) in saline (40–80 mM/L) at pH ~ 7.0 and room temperature (~20–22 °C) through the cochleostomy into the *Scala tympani* until all fluid was replaced by the solution. Excess liquid was allowed to overflow into the *Tympanic bulla*. Following a waiting time of 5–10 min, the *Tympanic bulla* was dried using absorbent swabs (Kettenbach GmbH & Co. KG, Eschenburg, Germany). Then the cochlea was slowly rinsed with Ringer's solution at room temperature to wash out the neomycin-sulfate. Afterwards excessive fluid was removed from the bulla. When deafening was performed after the electrode insertion into the midbrain, the deafening success was verified by the absence of acoustically evoked responses in the IC up to the highest sound pressure level tested (90 dB SPL_{rms}).

2.6. In vivo pressure measurements

The reversely transmitted pressure at the external ear canal was accessed during intracochlear optical stimulation at a wavelength of 1860 nm (Capella laser system) with various pulse durations. We surgically removed the pinna and placed a condenser microphone (1/4" microphone and Nexus amplifier, sensitivity 3.08 V/Pa, Brüel & Kjaer, Nærum, Denmark) over the cartilaginous external meatus and sealed it to the surrounding muscle by a rubber ring, allowing for pressure compensation (Fig. 1 C). The pressure was transformed into a voltage signal and recorded with a minimum sampling rate of 100 kHz. The reverse middle ear transfer function was not assessed during the experiments and the reported values were not adjusted for transmission loss.

2.7. Ex vivo pressure measurements

For comparison we performed *ex vivo* experiments to measure the laser-induced sound pressure in air (relative humidity 40–45%) and in the macerated guinea pig tympanic bulla (whole skull preparation). For the recordings in air, the tip of the optical fiber was placed ~600 μm off the middle and 2.5 mm below the microphone membrane with the fiber running perpendicular to the microphone. In the recordings from the macerated tympanic bulla, the optical fiber was inserted into the bulla through an artificial fenestration parallel to the cochlea and positioned perpendicular and close to the center of the outer ear-canal using a micromanipulator. The microphone was placed on the outer ear-canal and loosely sealed to the bone by a fitted rubber ring. For both *ex vivo* settings a variety of optical stimuli in the same range of parameters as in the *in vivo* experiments were applied and the resulting sound pressures were recorded.

2.8. Data analysis

All data was analyzed offline using custom programmed MATLAB R2012b (The MathWorks, Inc., Natick, Massachusetts, USA) routines. Multi unit activity (MUA) was analyzed by filtering the signal between 400 Hz and 3 kHz and extracting all samples as 'spikes' for which the amplitude exceeded the background by 3–4 times, depending on background noise level. Spontaneous spike rates were calculated in a 10 ms-time window before stimulus onset and the evoked spike rates were calculated using a time window of 15 ms after stimulus onset for tonal stimulation and 10 ms for click- and laser-stimulation, respectively. From the frequency tuning the cBF was calculated and the thresholds were visually determined and extracted from the data.

Spectrograms (2.5 ms Hamming window, 2 ms overlap; MATLAB signal processing toolbox, function: spectrogram) and power spectra (analysis restricted to pressure signal; MATLAB function: fft) were calculated from the pressure measurement data.

For statistical analyses data was tested for normal distribution using the Kolmogorov-Smirnov test. In all cases a normal distribution of the data could be verified and parametric tests were chosen to describe differences and correlations in the data. Where required the tests were corrected for multiple comparisons (Bonferroni correction). The test statistics are indicated in the text and figure legends for each case. For graphical representation mean and standard deviation were calculated and shown in the plots. For all tests p-values below 0.05 were considered significant.

3. Results

3.1. Intracochlear laser stimulation generated distinct pressure pulses at the external meatus

Initially, we aimed to characterize the acoustic properties of the laser generated sound. These were tested using microphone recordings at the external meatus during intracochlear optical stimulation (N = 7). We did not adjust the values according the reverse middle ear transfer function (Magnan et al., 1997, 1999, see discussion). The recordings provide access to the acoustic properties sounds induced intracochlearly. They revealed acoustic phenomena well above background noise level (Fig. 2). The wave form of the pressure pulse was stable with increasing stimulation level and only showed an increase in amplitude (Fig. 2 A). Some variability between subjects was observed (Fig. 2B–D), probably due to the position of the cochleostomy, bulla opening and other individual factors (see discussion). One common feature of the frequency-power-spectra calculated from the pressure recordings was high power for frequencies below 10 kHz and a substantial power drop-off above 10 kHz. Below 10 kHz several local power maxima were discernible. Typically these maxima did manifest at frequencies of approximately 2, 3.6, 6.3 and 8 kHz and at high stimulation levels (>250 mW pulse peak power) two additional local maxima between 15 and 20 kHz and between 25 and 30 kHz were apparent in 4 out of 7 cases. In contrast to the inter-individual differences between the pressure waves induced in different cochleae, only minor changes of wave form and frequency spectrum occurred for different stimulation-(fiber-) positions within each particular preparation (Fig. 2E–G). Even major changes in fiber position, e.g. irradiation through the

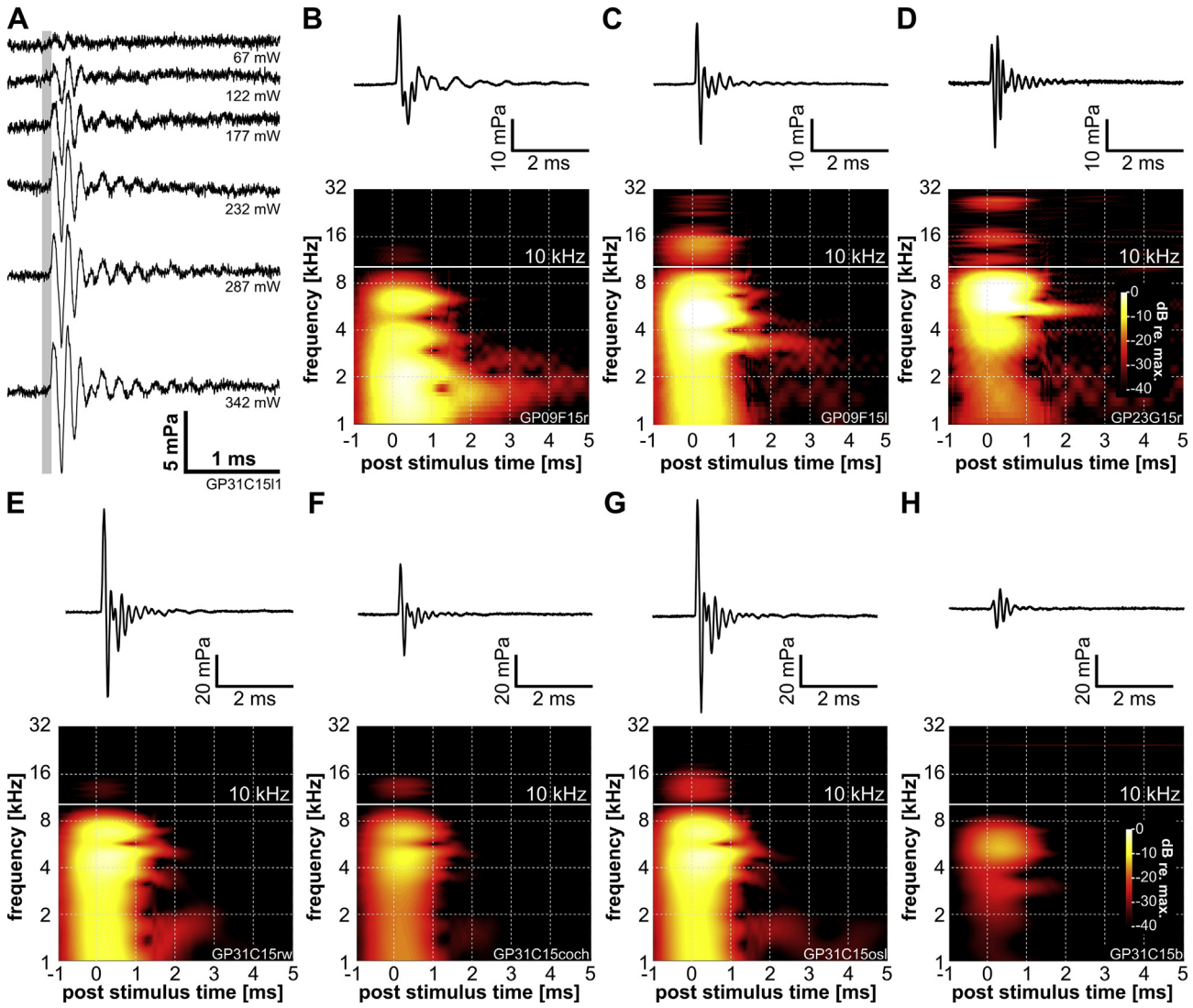

Fig. 2. Pressure pulses could be measured at the external meatus during intracochlear laser irradiation. **A**, The pressure pulses measured at the external meatus, in response to intracochlear NIR irradiation with 100 μs pulses of increasing pulse peak powers (≥67 mW; pulse energy: ≥ 6.7 μJ) are shown as oscillograms. The temporal structure of the pulse did not change with increasing pulse peak power. **B-D**, Temporal structure (top row) and the respective frequency distribution (lower row, spectrograms, power color coded, see D) varies between different subjects. However, we observed similar patterns, with a prominent power drop-off for frequencies >10 kHz in all cases. **E-G**, Intra-scalar NIR irradiation at different positions in a single preparation resulted in changes of the amplitude distribution, but not the overall temporal structure (top row) and frequency content (bottom row) of the pressure pulse recorded at the external meatus. Irradiation directed into the Scala tympani, towards the basilar membrane through the intact round window membrane (basal turn already cochleostomized, E) led to a pressure pulse with high power in frequencies below 10 kHz with a maximum close to 4 kHz. Intracochlear irradiation with a shallow insertion through the cochleostomy (F), just penetrating into the perilymph, resulted in a similar frequency distribution with less power below 10 kHz. For frequencies between 10 and 16 kHz a power increase is apparent compared to the irradiation through the round window. A deeper insertion through the cochleostomy, bringing the fiber tip into contact with the osseous spiral lamina (G) led to an overall increase in power. The frequency pattern remains stable, with a further increase in power between 10 and 16 kHz compared to the shallow insertion condition. **H**, an irradiation into the tympanic bulla, parallel to the cochlea, resulted in an altered frequency spectrum, with a maximum at approximately 6 kHz and reduced overall power. (E-H: power normalized to maximum power in G; B-H: wavelength: 1860 nm; pulse duration: 100 μs; pulse peak power: ~1 W). (For interpretation of the references to color in this figure legend, the reader is referred to the Web version of this article.)

(closed) round window membrane instead of intracochlear irradiation after insertion through a cochleostomy, resulted only in slight power-differences at any given frequency maximum. However, if the fiber was inserted into the tympanic bulla and pointed towards the outer bony wall of the cochlea, the spectral content of the recorded pressure pulse changed substantially, leaving only a single maximum between 4 kHz and 6 kHz (Fig. 2 H), a frequency that is close to the resonant frequency of the guinea pig bulla at approximately 4 kHz (Dallos, 1973). This indicates a less efficient energy transfer to the cochlea than by immersing the fiber in the perilymph or pointing it into the basal turn through the round window membrane.

3.2. Intra-collicular electrode position was verified by characteristic frequencies and thresholds

The electrodes used to record neuronal activity from the IC covered a recording depth of 1.5 mm with 16 electrode contacts. Along the penetration tracks cBFs between 0.5 kHz and 32 kHz were identified (Fig. 3 A). The majority of units (74%) had cBFs in the range between 5.7 kHz and 32 kHz (~2.5 octaves; Fig. 3 B, top). The median cBF values over all penetrations and animals ranged from 1.41 kHz at the most superficial electrode contact to 19.03 kHz at the deepest contact. The average lowest neuronal thresholds as a function of cBF resembled the behavioral

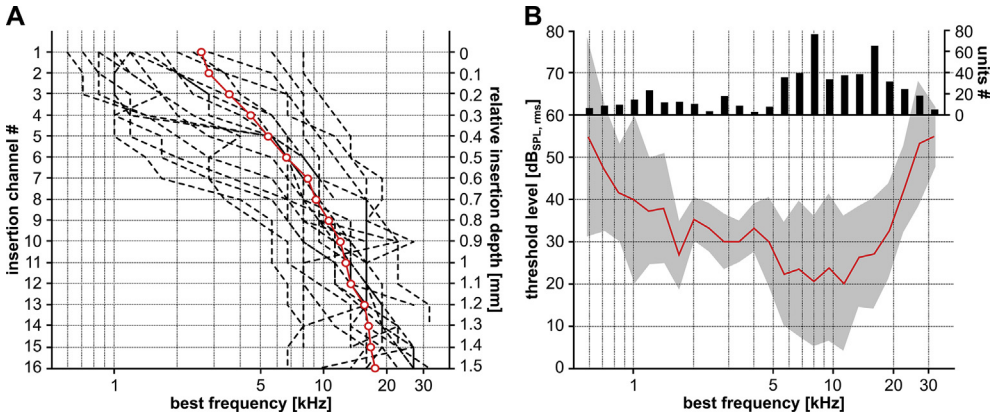

Fig. 3. Frequency sampling in the IC for all experiments. **A**, Typically, best frequencies (cBFs, abscissa) progressed from low to high frequencies along recording positions in the IC (ordinate). Dashed lines indicate frequency progressions over more than 5 subsequent contacts along a single shank of an electrode array for 20 animals (572 responsive recording sites, for double shank penetrations the electrode track with the broadest frequency coverage is shown). Median frequencies at each electrode position are potted in red for all cases. **B,** The average thresholds (red line, grey area indicates standard deviation) are plotted over cBF for all cases shown in A (for repeated cBFs in a single recording track only the lowest threshold was kept). The number of units per cBF is shown as histogram at the top of the graph. Of all units sampled 74% had cBFs above 5 kHz. (For interpretation of the references to color in this figure legend, the reader is referred to the Web version of this article.)

audiogram described for the guinea pig (Heffner et al., 1971) reduced in sensitivity by approximately 10 dB (Fig. 3 B), comparable to the findings in the guinea pig IC in earlier studies (Syka et al., 2000). Thus, the frequency range covered by recordings in this study corresponds to the cochlear frequency map including all optical stimulation sites accessible through a cochleostomy and extending well beyond the basal turn (Viberg and Canlon, 2004).

3.3. IC recordings corresponded to pressure measurements

The peak pressure recorded at the external meatus during intracochlear laser stimulation increased linearly with the pulse peak power of the laser output (Fig. 4 A). The resulting logarithmic growths of sound pressure levels with increasing pulse peak power was similar to that measured along the beam path in humid air and that recorded at the bony external meatus of a macerated skull during NIR laser irradiation in the bulla. Consequently the growth function of maximum spike rates in the IC with increasing pulse peak power closely resembled growth function of the sound pressure level (Fig. 4 B). By plotting the same spike rate data as a function of the sound pressure level recorded at the external meatus, a linear growth of spike rate with increasing peak sound pressure level becomes apparent (Fig. 4 C). It indicates that the observed spike rates in the IC are linearly correlated with the optoacoustically generated sound pressure level, while the generated pressure is linearly correlated to the pulse peak power of the optical stimulus. This points to a purely passive stimulation mechanism based on energy absorption in the cochlea during NIR irradiation without direct activation of auditory nerve fibers.

Additional to an increase in spike rate correlated with an increase in pulse peak power, we also observed an expansion of the IC response to regions with higher cBF. This frequency expansion was consistent with a broadened frequency spectrum above the noise floor at increased stimulus power (Fig. 5A–C). In contrast to these

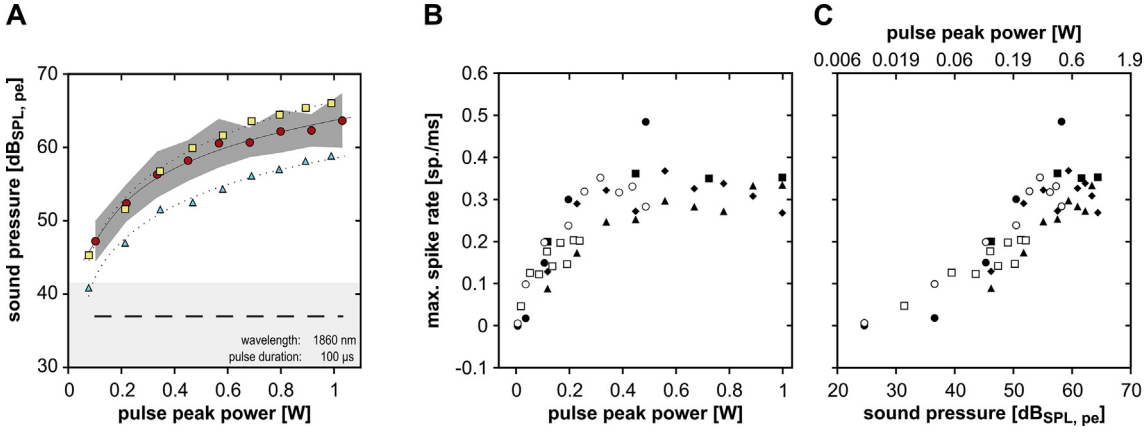

Fig. 4. Sound pressure level at the external meatus and response strength in the IC correlated with pulse peak power of the NIR laser pulse. **A**, The average peak sound pressure level (ordinate) recorded at the external meatus increased with increasing pulse peak power (abscissa, n = 7, red circles, gray area represents standard deviation). The sound pressure level increased from 48 dB peSPL at 0.06 W to 63 dB peSPL at the laser output maximum at ~1 W (thick dashed line marks the noise floor of the microphone). This sound level increase is comparable to that recorded perpendicular to the beam path in air (blue triangles) and at the bony meatus of a macerated skull during irradiation in the tympanic bulla (yellow squares). **B**, In five cases, where IC recordings were combined with pressure recordings at the external meatus, the maximum spike rates (independent of tonotopic recording position) during intracochlear NIR stimulation were recorded (different cases indicatet by different symbols). The increase in spike rates correlated with increasing pulse peak power in a similar manner as the peak sound pressure levels in A. **C**, The same data as in B plotted over peak sound pressure levels revealed a good correlation ($r^2 = 0.76$ for a linear regression) between the sound pressure induced by intracochlear laser irradiation and maximum spike rates (pulse peak power axis adjusted to the sound pressure axis shown at top). (For interpretation of the references to color in this figure legend, the reader is referred to the Web version of this article.)

findings, an increase in pulse energy by varying pulse duration, at constant pulse peak power, led only to slight variations of the frequency spectrum of the pressure pulse and the IC response pattern, respectively (Fig. 5D–F). These differences can be attributed to variations of the temporal structure of the pressure response due to changing pulse durations. Despite these spectral differences, the evoked neuronal response typically lasted 5 ms, irrespective of stimulus parameters. Within the inherent physical limitations, resulting from the interconnectedness of the stimulus parameters pulse peak power, pulse energy and pulse duration, the results described above and shown in Figs. 4 and 5 suggest that the response strength in the IC depends on the sound level of the optoacoustically generated pressure and thus is connected to pulse peak power (Fig. 4A).

3.4. Inferior colliculus units did not respond to intracochlear NIR stimulation in deafened animals

We investigated the contribution of direct neural stimulation by laser irradiation of primary cochlear structures (n = 10 animals). For this goal we recorded the responses to intracochlear laser stimulation before and after deafening by an intra-scalar infusion of neomycin-sulfate-solution (2.5–5% in Ringer's solution). We tested optical pulses with durations of either 5 ns at a wavelength of 1850 nm (8 penetrations in 4 animals), or with 100 μs duration (12 penetrations in 6 animals) at a wavelength of 1860 nm both with pulse energies of 6 μJ.

While IC responses could reliably be evoked for both pulse types in hearing animals, we did not observe any responses after acute pharmacological deafening (Fig. 6). However, the spiral ganglion cells remained responsive to electric stimulation at current levels typical for acutely deafened guinea pigs (237.14 μA ± 3.6 dB, compare Sato et al., 2016; Miller et al., 1993, 1995, 1998). On average, the mean maximal instantaneous spike rate in response to electric stimulation (0.84 spikes/ms), close to stimulation threshold (+1 dB), was approximately 80% higher than the mean maximum spike rate (0.47 spikes/ms, Fig. 6 B) evoked by pulsed laser stimulation with a pulse peak power of 60 mW (100 μs pulse duration). Additionally, the cBFs of units responding strongest to electric stimulation in the deaf ear were higher than (or in two cases equal to) those of units responding strongest to optical stimulation in the hearing ear, while the opposite was never observed (Fig. 6 C). This indicates that generally, optical stimulation evokes responses at sites apical to the fiber location.

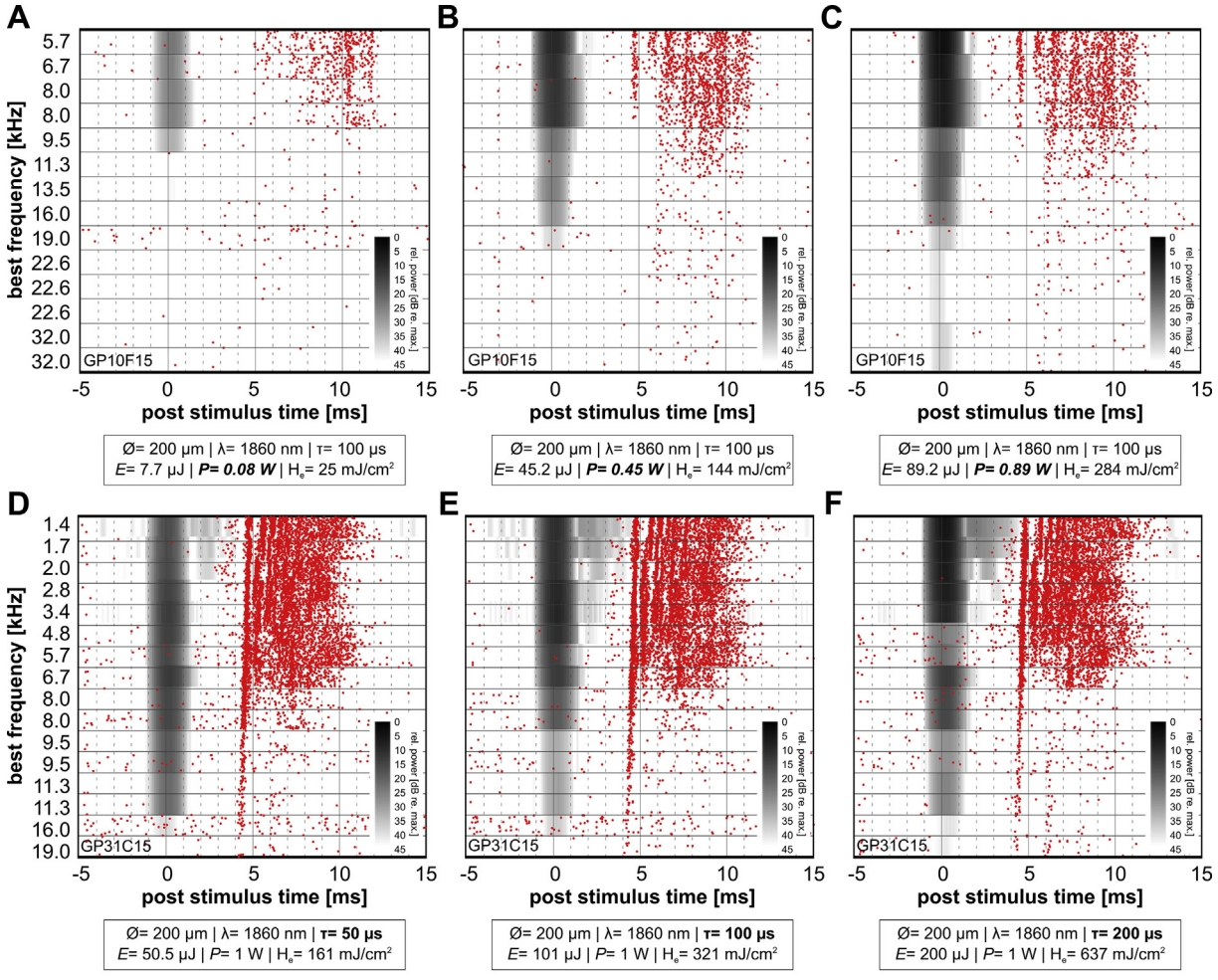

Fig. 5. Excitation spreads with increasing pulse peak power and is irrespective of pulse energy. **A-C**, With increasing pulse peak power (A to C) neural activity spreads along the tontopic axis of the IC from low frequencies (ordinate, A) to higher frequencies (C, activity shown for 100 stimulus repetitions, red dots symbolize multi unit spikes). The spread follows the power spread of the respective spectrograms (gray shaded area centered on stimulus onset, frequencies matched to the cBFs of the IC recording). **D-F**, Increasing the pulse energy at stable pulse peak powers, by varying the pulse duration from 50 μs (D) to 200 μs (F), did not result in changes in activity and spread along the IC tonotopic axis. The slight variations in power along the frequency axis due to the different pulse durations have little effect on the spiking behavior (activity shown for 100 stimulus repetitions). (A-F: fiber diameter, wavelength, pulse duration, pulse energy, pulse peak power and radiant exposure values are noted below figures). (For interpretation of the references to color in this figure legend, the reader is referred to the Web version of this article.)

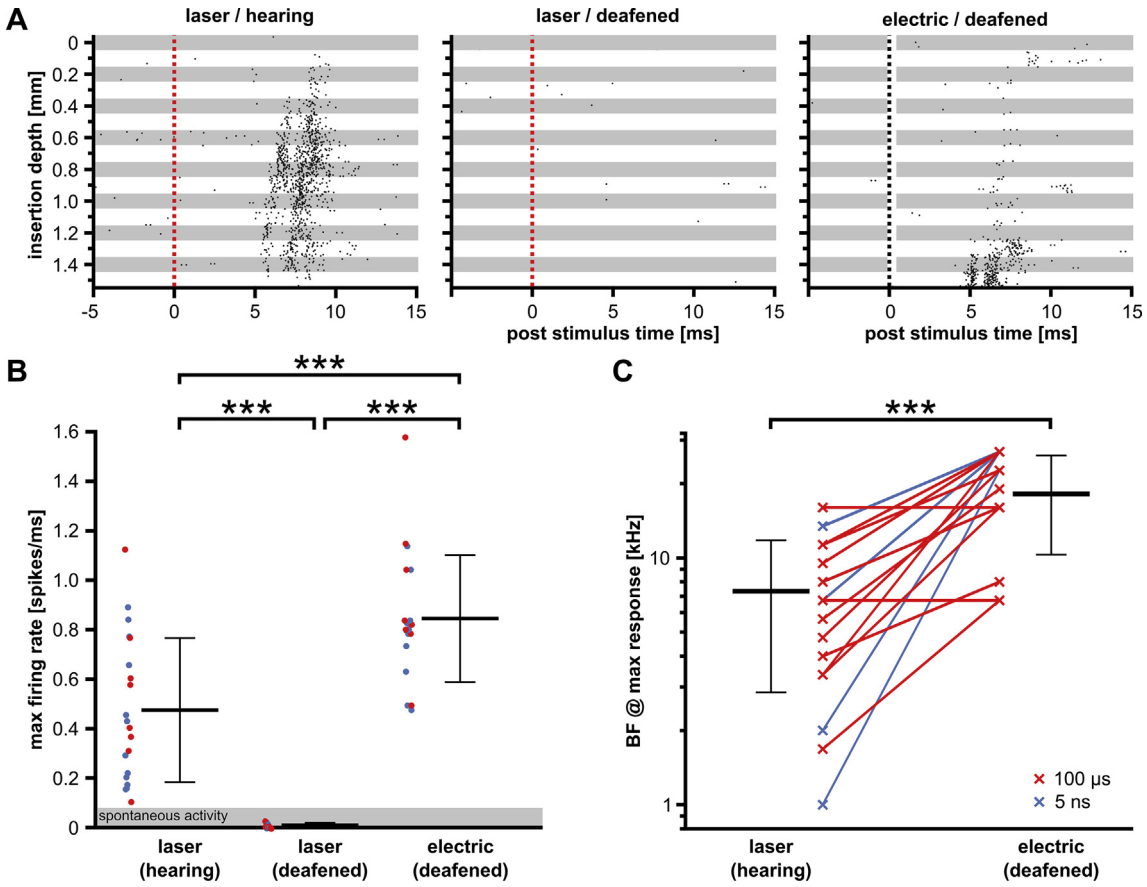

Fig. 6. No IC responses can be optically evoked in deaf animals. **A**, In this typical raster plot example, multi unit activity (MUA, each point represents one spike) over time (abscissa) is plotted in relation to the length of the electrode array (ordinate, insertion depth relative to first contact), the stimulus onset is indicated by dashed lines. The most pronounced IC activation occurs in the middle of the electrode array during optical stimulation (100 µs pulse) of the normal hearing animal (left). After deafening no response above background activity can be evoked by optical stimulation (middle). An electric stimulation close to threshold level (threshold + 1 dB) evokes a clearly discernible activation at the deepest electrodes in the array (right, stimulus artifact blanked). **B**, This whisker-plot illustrates the maximum firing rates of IC units in response to intracochlear NIR-stimulation before and after deafening and firing rates in response to electrical stimulation at 1 dB above the electric stimulation threshold. The data for µs and ns NIR-pulses were combined, as no significant difference between maximum firing rates and variance of these groups were observed (100 µs, 6 µJ NIR pulses: 12 penetrations in 6 animals, blue; 5 ns, 6 µJ pulses: 8 penetrations in 4 animals, red). Firing rates in response to optical stimulation dropped to the spontaneous level after pharmacological deafening, while an intracochlear electric stimulation at the position of the optical fiber tip resulted in a robust activation of IC neurons. The firing rates evoked by electric stimulation at 1 dB above threshold were significantly higher than the responses to NIR stimulation. (*** $p < 0.00033$; pairwise students t-test, two tailed, corrected for multiple comparisons) **C**, Maximum spike rates during electric stimulation typically occur at electrode positions with higher cBF (ordinate) than during optical stimulation (abscissa, same data as in B, only highest instantaneous spike rates per penetration and animal are shown, 100 µs pulses: blue; 5 ns pulses: red). Electric stimulation in deaf animals (compare B) evoked maximum spike rates at deeper electrodes in the IC with significantly higher cBF than optical stimulation. (*** $p < 0.001$; pairwise students t-test, two tailed). (For interpretation of the references to color in this figure legend, the reader is referred to the Web version of this article.)

3.5. Response patterns in the IC are similar for various optical stimulation parameters

Additionally we stimulated sequentially using the nanosecond laser system at 6 µJ pulse energy and ranging from visible light (434 nm) to upper NIR range (1961 nm) and the microsecond laser system at a fixed NIR wavelength (1860 nm) and with various pulse durations ranging from 10 µs to maximally 20 ms ($n = 6$). All stimuli led to an activation of IC neurons in similar cBF ranges and with similar latencies and response durations. The response strength showed slight variations depending on the stimulation parameters.

Overall, we found similarities across activation patterns for different laser-stimuli in all recordings (Fig. 7A–C). Units with low acoustic response thresholds did respond well to optical stimuli at NIR wavelength in both the microsecond and nanosecond range and visible light in the nanosecond range. Units with response thresholds between 30 and 40 dB SPL_{rms} responded best when their cBFs were below 10 kHz. Another common feature of the responses was less excitation of low cBF (<5 kHz) units by nanosecond pulses than by microsecond pulses (compare Fig. 7 A and C). However, electric stimulation (Fig. 7E and F) revealed apparent differences in the activation patterns compared to both acoustic clicks (Fig. 7 D) and optical stimulation (Fig. 7A–C): strong activation for units with cBFs above 10 kHz, independent of the acoustic stimulation threshold. At higher electric stimulation levels, the activity did spread to units with lower cBFs (threshold +3 dB, Fig. 7 F). Overall the IC activation by intracochlear NIR stimulation resembled evoked acoustic click responses besides less activation above 10 kHz. This again points to an optoacoustic origin of the responses.

3.6. Pressure spectra and IC response distribution indicated a global cochlear activation by optical stimulation

Finally, we pooled the responses of all 496 acoustically characterized IC units to intracochlear 100 µs NIR stimulations at various pulse peak powers ($n = 2096$) from all animals with this type of stimulation and recording ($n = 17$) to provide a global response-

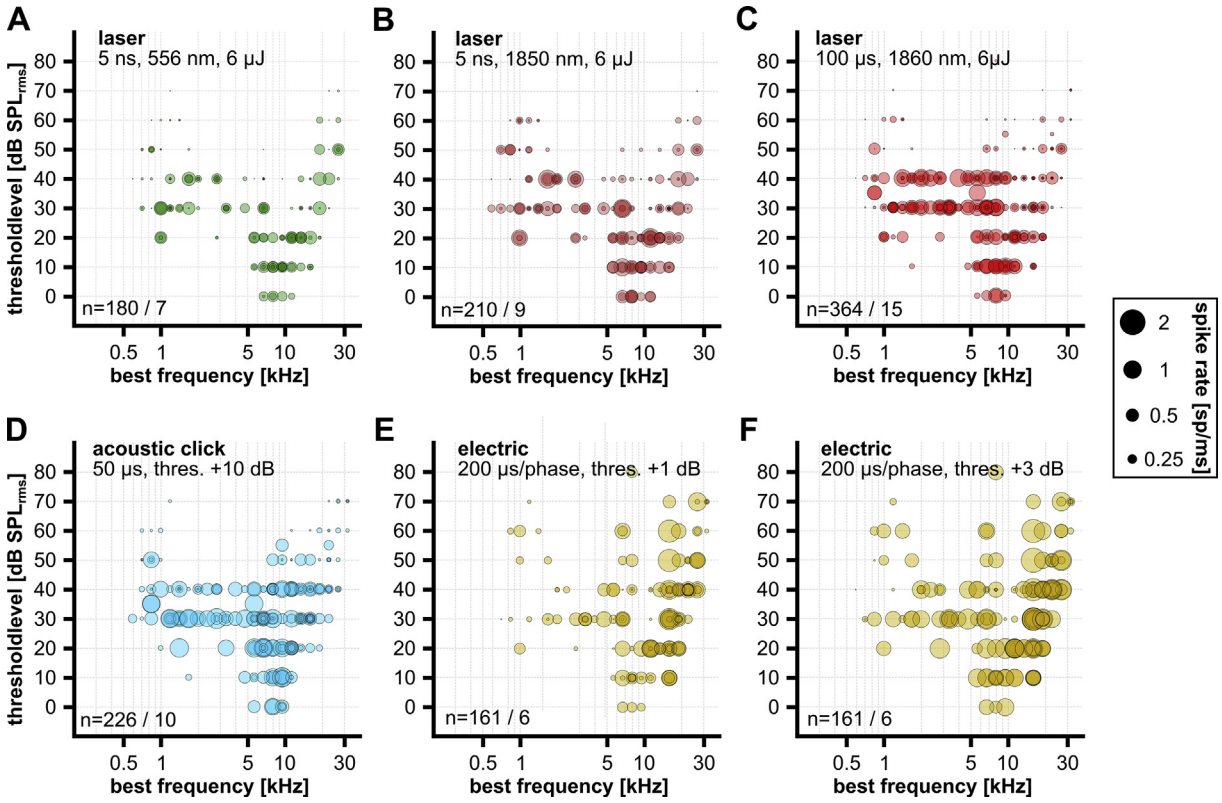

Fig. 7. Group responses in the IC evoked by optical stimulation are similar to click-evoked responses, but distinct from electrically evoked responses. All IC units studied were characterized by their best frequencies (x-axes) and response thresholds to pure tone stimulation at cBF (y-axes) to pure tone stimulation and plotted into a gross IC response map. Given are the response-strengths (spike rate, circle area) to optical stimuli, acoustic clicks and electric pulses, respectively. **A,** The spike rates in the IC were highest in units with thresholds of ≤30 dB SPL_{rms} during stimulation with ns-pulses of visible light. **B**, NIR stimulation with ns-pulses resulted in a stronger activation but with overall response characteristics similar to A. **C**, During stimulation with µs-pulses, IC units with thresholds ≤50 dB SPL_{rms} had high spike rates with a somewhat less pronounced flank at high cBF units, than in A and B. **D**, Stimulation with acoustic clicks at 10 dB above the absolute response threshold, resulted in a homogeneous activation of IC units. **E** and **F**, in contrast to A - D, an electric stimulation in the cochleae of deafened animals activates units that had threshold levels of up to 70 dB SPL_{rms} during pure tone stimulation in hearing condition, but mostly at frequencies above 10 kHz. These responses were even stronger at high cBF further from threshold (threshold + 3 dB, F). The numbers at the top of each plot indicate the number of units and animals, respectively.

overview. In direct comparison, the cumulated IC responses of all recordings were significantly correlated (Spearman correlation of mean spike rate and mean signal power at the external meatus at the same frequency as unit cBF, two tailed, $r = 0.8325$, $p < 0.0001$) with the average power spectrum of the pressure recordings at the external ear (Fig. 8 A, top). Overall ~56% of the IC units with cBFs below 10 kHz ($n = 318$) were responsive to intracochlear NIR stimulation, a frequency range where the NIR-evoked sound had the highest spectral power (Fig. 8 A, bottom). In this range spike rates up to 1 sp/ms were measured. While some IC units with cBFs beyond 10 kHz had relatively low acoustic response thresholds (compare thresholds in Fig. 3 B), the maximum spike rates did not exceed 0.7 sp/ms and only ~25% of these units ($n = 178$) were responsive to intracochlear NIR stimulation. In the pressure power spectrum a side maximum was commonly found in this range (see Fig. 2C and D). Only a fraction of ~6% of units with cBFs above 20 kHz ($n = 47$) responded to intracochlear NIR stimuli. The spectral power of the NIR-evoked sound in this frequency range was close to the background noise level.

We projected the IC response strengths onto their putative place of origin according to their cBF and the frequency-place map of the guinea pig (Viberg and Canlon, 2004; Greenwood, 1990) in a generic 3 dimensional model of a left guinea pig cochlea (computed from µCT data of a macerated skull specimen, Fig. 8 B). This projection revealed that the majority of responding units (85%) and the responses to various optical stimuli (72% of spike rates above spontaneous rates; $n = 1562$ stimulations), especially the strongest ones (94% of responses exceeding 0.3 sp/ms; $n = 204$ stimulations), originated outside of the reach of the optical fiber and the respective direct NIR beam path (lateral half of the basal turn; ~33% of the overall cochlear length; CF > 12 kHz). Responses could be observed in units with cBFs below 1 kHz, far apical from the stimulation site. In contrast, over 50% of IC units activated by electric stimulation close to threshold ($n = 147$) had cBFs corresponding to locations in the basal turn of the cochlea (Fig. 8 C). The spike rates evoked by NIR-stimulation neither correlated significantly with spike rates evoked by electric stimulation at 1 dB above stimulation threshold (Spearman correlation, two tailed, $r = -0.2636$, $p < 0.2482$) nor at 10 dB above threshold (Spearman correlation, two tailed, $r = -0.1429$, $p < 0.5367$). These results further support a global cochlear activation by optical stimulation, likely by optoacoustics, rather than a spatially restricted direct activation of neural elements or hair cells along the beam path.

4. Discussion

The present study defines the acoustic features of pressure pulses induced by laser irradiation in the hearing guinea pig cochlea. The neural response characteristics recorded from the auditory midbrain are corroborated by the pressure levels and spectral characteristics measured at the external ear. Sound pressure levels at the external ear reached up to 70 dB peSPL. Pressure

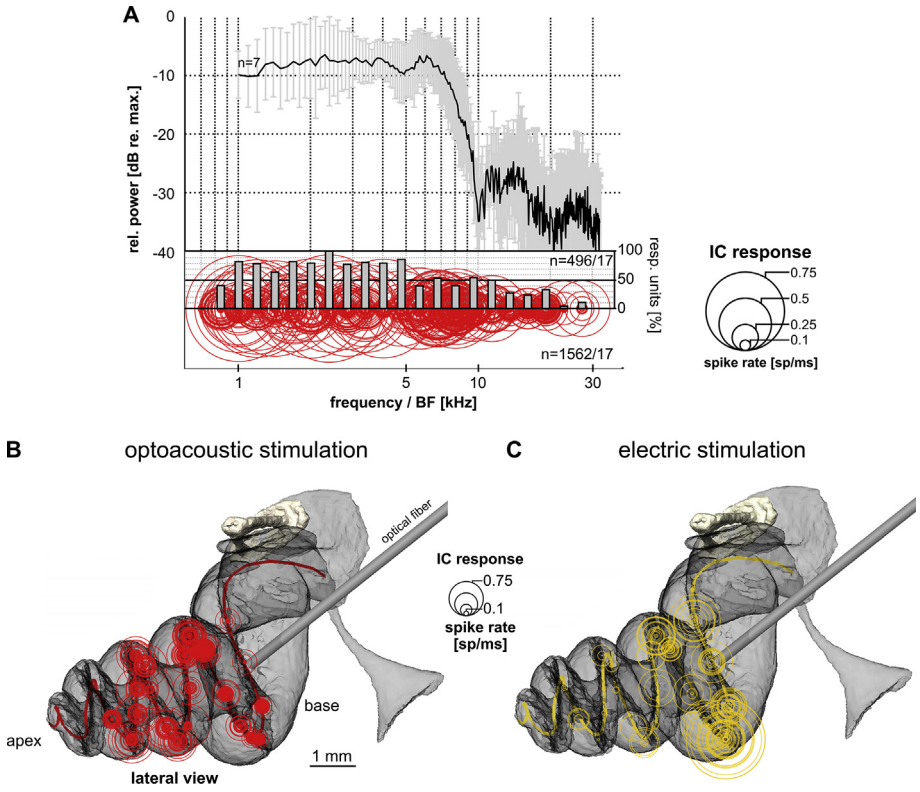

Fig. 8. External pressure measurements and IC response patterns revealed a broad intracochlear activation by laser stimulation. A, In the average power spectrum of 7 pressure measurements at the external meatus (black trace at the top, gray error bars are standard deviation), the power drop-off at frequencies above 10 kHz is the most prominent feature (compare Fig. 2). No spectral fine structure is preserved below 10 kHz, partly due to differences between preparations, however, between 10 and 16 kHz and between 24 and 30 kHz two local power maxima are discernible. The response strengths at cBFs between 0.5 and 32 kHz in the IC (spike rate proportional to the area of the red circles) for 2096 recordings during intracochlear NIR stimulation (1860 nm, 100 µs) at various pulse peak powers (~0.006 W - 1 W) in 17 animals (bottom plot) correspond to the spectral power of the sound generated by the laser stimulus. All units identified in the IC (regardless of threshold level, response pattern or response strength) are combined in the plot. The proportion of units at each cBF that did respond to optical stimulation is overlayed as histogram (gray bars, response > 5% of the pure tone maximum). Units with lower cBFs had a higher probability of responding. B, A projection of the IC responses (red circles) according to their cBF onto a reconstruction of the guinea pig cochlea (µCT) reveals strong responses throughout the cochlea even though the fiber (shown schematically at one putative position) reached only the basal half turn of the cochlea (frequency position reconstruction according to Greenwood-function parameterized as follows: F = 0.5*(102.1*(x/20.58)-1) (Viberg and Canlon, 2004), scale refers to B and C). C Compared to optoacoustic stimuli, electric stimulation at the fiber tip at 1 dB above threshold (n = 147 in 6 animals) mostly lead to a midbrain activation corresponding to the basal cochlear turn (yellow circles). (For interpretation of the references to color in this figure legend, the reader is referred to the Web version of this article.)

measurements and the dominant neural activation at cBFs between 1 and 10 kHz indicate an excitation of cochlear regions apical to the stimulation site, not directly accessible by NIR irradiation. Concordantly, no neuronal responses could be evoked by optical stimulation in deafened animals, while electric stimulation of the deafened ear was possible and predominantly resulted in an activation of units with higher cBFs at threshold, indicating the fiber position. These findings demonstrate the absence of any noteworthy direct neural stimulation. Overall our results reveal an optoacoustic origin of the cochlear excitation in hearing conditions. The optoacoustic stimulation may be suitable and loud enough for an application in implantable hearing aids and hybrid electro-optoacoustic devices to drive residually hearing portions of the cochlea (for details see below).

4.1. Relation between intracochlear stimulation sites and IC recordings

The cochleostomic access enabled an optical stimulation of the cochlea in the lateral half of the basal turn of the guinea pig cochlea. Thus, according to the Greenwood function of the guinea pig, cochleotopic positions between approximately 8 kHz and 40 kHz could be directly accessed with an optical fiber (Viberg and Canlon, 2004; Greenwood, 1990). The fiber was located in the basal-most cochlear halfturn. We therefore assume that cochleotopic positions below 8 kHz remained inaccessible to the light beam. The cBFs of all units identified in the IC ranged from approximately 0.6 kHz–32 kHz. This represents a typical range for recordings from the IC in guinea pigs (Sato et al., 2016; Richter et al., 2011b; Snyder et al., 2008). The tonotopic range of identified cBFs for units responding to optical stimulation extended from the basal turn to the 3rd turn of the guinea pig cochlea (Viberg and Canlon, 2004). This is beyond all putative optical stimulation sites that could be accessed by an optical fiber insertion through a cochleostomy at the cochlear base. This indicates that the response to pulsed laser light is predominantly optoacoustic.

4.2. Effect of deafening

Acute deafening by intra-scalar infusion of neomycin sulfate solution (2.5–5%) abolished all responses to acoustic stimulation, within minutes after infusion (compare Snyder et al., 2004; Middlebrooks and Bierer, 2002; Miller, 2001; Leake-Jones et al., 1982). In the current study, neomycin infusion was performed at the end of the experiments, with approximately 2 h of recordings after deafening, sufficient for data collection but too brief for allowing functional effects of neomycin on SGNs (Leake-Jones et al., 1982). Supporting this, electric stimulation at current levels that

were in a typical range for acutely pharmacologically deafened guinea pigs (Sato et al., 2016; Snyder et al., 2004, 2008; Miller et al., 1993, 1998) resulted in the expected responses and confirmed the good function of the auditory nerve.

While IC responses to intracochlear NIR stimulation could reliably be evoked prior to deafening, we did not find spike rates exceeding spontaneous activity after deafening. The electric stimulation current was delivered through an electrode at the tip of the optical fiber. The activation of high cBF units in the IC in response to electric stimulation close to threshold level can be attributed to the corresponding frequency of the intracochlear location of the fiber (Sato et al., 2016; Snyder et al., 2008). In contrast, the stimulation of the hearing cochlea by NIR laser pulses was not spatially restricted to the position of the fiber tip. It has been suggested that the laser beam might stimulate SGNs in neighboring cochlear turns apical to the intracochlear fiber position along the beam path (Moreno et al., 2011). But even taking these considerations into account, we did not find any indication for an excitation exclusively along the beam path from the estimated fiber position. Taken together with the acoustic properties of the NIR-evoked sound and the cBFs of units sensitive to NIR-stimulation, these results demonstrate an optoacoustic origin of the responses during intracochlear laser stimulation in absence of any significant signs of direct stimulation of SGNs or auditory. This is consistent with only minimal signs of depolarization, well below spiking threshold, in isolated SGC in vitro during pulsed laser stimulation (Rettenmaier et al., 2014). We therefore assume that direct neural stimulation is no confounding factor during optoacoustic stimulation through the technique presented here.

4.3. IC responses to intracochlear laser stimulation

The activation patterns in the IC during intracochlear optical stimulation are similar regardless of wavelength and pulse duration of the optical stimulus. This could be observed in the spatio-temporal activation patterns of individual recordings and the overall IC response pattern. The patterns were distinct from those during monopolar, single-pulse electric stimulation, but similar to those during acoustic click stimulation, yet with less activation above 10 kHz. We observed only minor differences in response patterns for visual wavelength stimulation and NIR stimulation despite large differences in penetration depth in aqueous environments (Palmer and Williams, 1974; Hale and Querry, 1973) and an energy absorption in different tissues (Schultz et al., 2012). The observation that pulse peak power rather than pulse energy can explain the observed response strengths, further corroborates the optoacoustic origin of the pressure wave in the lymphatic fluids of the inner ear, in accordance with earlier studies (Kallweit et al., 2016; Schultz et al., 2014). The lack of spatial selectivity of the optic stimulation also speaks against a direct displacement of the basilar membrane by the laser pulse, a possible stimulation mechanism that had been discussed earlier (Schultz et al., 2012). Furthermore, different fiber positions also resulted in only minor changes of the IC response pattern in hearing animals. This finding points to a universal stimulation mechanism that is independent of the place of absorption. One such mechanism could e.g. be a resonance phenomenon within the temporal bone and the bulla driven by vibrations due to the fast energy deposition into the cochlear fluid volume.

4.4. Characteristics of the sound recorded at the external meatus

The sound spectra recorded at the external meatus during optical stimulation differed between preparations. Yet for any given preparation they remained unchanged for different intracochlear fiber positions and even for a laser irradiation of the basal cochlear turn through the closed round window membrane. The reverse transfer function of the guinea pig middle ear is relatively flat up to 10 kHz (Magnan et al., 1997). Therefore the sound spectrum below 10 kHz mirrors the intracochlear pressure spectrum well, but attenuated by approximately 30 dB. Beyond 10 kHz a certain risk of misestimating the intracochlear pressure is given (Magnan et al., 1999) and the recorded values have to be carefully interpreted.

If the fiber position in the tympanic bulla was pointed towards the outer bony wall of the cochlea, the spectrum exhibited only a single maximum at 5.6 kHz (Fig. 6 H) which is close to the resonance frequency of the guinea pig bulla (Dallos, 1973). This suggests a stimulation mechanism based on resonance of the space in the bulla. That could be influenced by the exact position of the cochleostomy, interindividiual differences in cochlear anatomy and probably also the size and position of the bulla opening, thus explaining the differences between different preparations. Overall the data indicate a higher efficiency of optoacoustic stimulation when the optical energy is delivered directly into the cochlea compared to the tympanic bulla. The growth function of the sound level recorded for different optical stimulation parameters again points to pulse peak power as the determining factor. The maximally determined extracochlear sound pressure level for single 100 μs pulses was 70 dB peSPL (at 1 W pulse peak power), which indicates intracochlear pressure levels of 100 dB SPL or more considering the reverse middle ear transfer function of the guinea pig (Magnan et al., 1997, 1999). Xia et al. (2016) recorded the pressure directly within guinea pig cochleae in cadaveric as well as in two *in vivo* preparations. They reported an intracochlear pressure of approximately 100 dB SPL during NIR stimulation at parameters similar to those reported here. A pulse with 100 μs duration and a peak power of 1 W corresponds to a pulse energy of 100 μJ and a radiant exposure of 320 mJ/cm^2 for a fiber diameter of 200 μm about half of the damage threshold for single pulses reported elsewhere (Wells et al., 2007b) for a wavelength 2120 nm. While the safety for pulse trains will have to be evaluated in future, this indicates that the pulses used in this study are sufficiently strong and save for use in “optoacoustic hearing aids”.

4.5. Comparison between external meatus sound recordings and IC responses

The comparison between the sound pressure recordings and the IC responses reveals a good agreement between both measures. The increase in spike rate observed in the IC for pulses of increasing pulse peak power can be explained by the increase in sound pressure level, as recorded at the external meatus. The spike rates of units in the IC also correlated significantly with the spectral power at frequencies corresponding to their respective cBFs for sound recordings at the external meatus. Even taking into account uncertainties about the intracochlear pressure above 10 kHz in the reverse middle ear transfer function (Magnan et al., 1997, 1999), the responses in the IC below this frequency can reliably be explained by an NIR induced optoacoustic pressure in the cochlea. There are apparent differences to the power spectrum acquired from intracochlear pressure measurements during intracochlear NIR in the guinea pig by Xia et al. (2016). The spectrum reported there had a prominent single peak above 20 kHz. In contrast, pressure recordings in the external meatus (Xia et al., 2016) resulted in a similar power spectrum as reported in the present study with a pressure increase below 10 kHz and a side peak at ~15 kHz. This shows the low-pass filter characteristic of the middle ear with the ossicular chain during reverse transmission. Therefore it needs to be considered that our method is not sensitive enough to reliably

capture spectral components of the NIR induced sound beyond 20 kHz. However, the neural responses recorded in the IC mirrored the increased spectral power below 10 kHz, while only few responses were recorded from units with cBFs above 20 kHz. In any case the presence of an acoustical high frequency component would not serve as a confound to optoacoustic stimulation of cochleae with residual function only in low frequencies. While this difference between intracochlear pressure measurements and measurements in or at the external meatus would warrant further investigations, we can exclude a confounding direct neural stimulation of the basal, high frequency region of the cochlea because the optoacoustically evoked responses did not correlate with those evoked by electric stimulation in the basal turn.

The IC response strength depends on pulse peak power rather than on pulse duration and with that pulse energy, corroborating the findings of Kallweit et al. (2016) who showed that the laser induced pressure depends on the 1st derivative of the optical power. This means that sufficiently high sound pressures for intracochlear optoacoustic stimulation could potentially be reached through modulating the pulse peak power of short pulses, thus keeping the pulse energy low. This could facilitate the heat dissipation between the pulses in order to avoid intracochlear heating for a stimulation with pulse trains (Thompson et al., 2012). With sufficiently high repetition rates it could be possible to transfer envelope information of an acoustic signal. A first simulation of such an envelope transfer by optoacoustic stimulation was successfully tested in EAS users (Krüger et al., 2017).

Despite such promising first results, the applicability and safety of optoacoustic stimulation for EAS needs careful investigation. Considering the repetition rates necessary for an optoacoustic transfer of envelope information, the lowered damage threshold compared to single pulses needs to be considered (Wells et al., 2007b). Also heat accumulation and dissipation has to be investigated. It has been suggested that heat dissipation is fast enough to avoid a decrease of neural responses over time for repetitions rates lower than 250 Hz and radiant energies below 30 μJ/pulse and no structural damage was observed in the guinea pig cochlear after a long term exposure with 127 μJ/pulse at repetition rates of 250 Hz (Goyal et al., 2012), a value slightly above the maximum of 100 μJ/pulse used in the current study. Whether or not this is safe for application in human users needs to be the focus of future investigations. In the present study we could show that stimulation through the intact RWM could be feasible. Leaving the optical stimulation device out of the lymphatic space of the cochlea might help to stay within temperature safety limits for pulse trains fast enough to carry acoustic envelope information.

5. Conclusions

In this study we provide evidence for the feasibility of optoacoustic intracochlear stimulation. With the parameters tested here we saw a considerable activation of frequency regions apical to the stimulation site. We further could show that a direct stimulation of primary auditory structures by NIR pulses can be excluded as confounding stimulation mode in such an approach. The optical energy could be delivered through a single channel and be modulated to transmit envelope information to functioning apical regions of the cochlea. This appears to be possible for a stimulation through the closed round window membrane. Further study is needed to determine, whether this approach of an “optical actuator” could potentially be combined with a conventional CI for electric stimulation to provide combined EAS stimulation from a single device in the future.

Funding

Supported by Cluster of Excellence Hearing4All (DFG-EXC 1077), EU ACTION (FP7 ICT project 611230) and MedEl Company, Innsbruck, Austria.

Appendix A. Supplementary data

Supplementary data to this article can be found online at https://doi.org/10.1016/j.heares.2018.11.003.

References

Dallos, 1973. The Auditory Periphery: Biophysics and Physiology. Academic Press, New York.
Duke, Cayce, Malphrus, Konrad, Mahavaden-Jansen, Jansen, 2009. Combined Optical and Electrical Stimulation of Neural Tissue in Vivo, vol. 14, pp. 25–27 (6).
Goyal, Rajguru, Matic, Izzo, Stock, Richter, 2012. Acute damage threshold for infrared neural stimulation of the cochlea: functional and histological evaluation. Anat. Rec. 295 (11), 1987–1999.
Greenwood, 1990. A cochlear frequency-position function for several species–29 years later. J. Acoust. Soc. Am. 87 (6), 2592–2605.
Guan, Wang, Yang, Zhu, Wang, Nie, 2016. Near-infrared laser stimulation of the auditory nerve in Guinea pigs. J. Opt. Soc. Korea 20 (2), 269–275.
Hale, Querry, 1973. Optical constants of water in the 200-nm to 200-μm wavelength region. Appl. Optic. 12 (3), 555.
Heffner, Heffner, Masterton, 1971. Behavioral measurements of absolute and frequency-difference thresholds in Guinea pig. J. Acoust. Soc. Am. 49 (6), 1888–1895.
Kallweit, Baumhoff, Krüger, Tinne, Kral, Ripken, et al., 2016. Optoacoustic effect is responsible for laser-induced cochlear responses. Sci. Rep. 6 (5092), 28141.
Konerding, W.S., Froriep, U.P., Kral, A., Baumhoff, P., 2018. New Thin-Film Surface Electrode Array Enables Brain Mapping with High Spatial Acuity in Rodents. Sci. Rep. 8 (1), 3825.
Krüger, Fiedler, Baumhoff, Shah, Kral, Büchner, et al., 2017. Model based laser stimulation for speech coding in Cochlear Implant users with low frequency residual hearing. In: CIAP. Lake Tahoe.
Leake-Jones, Vivion, O'Reilly, Merzenich, 1982. Deaf animal models for studies of a multichannel cochlear prosthesis. Hear. Res. 8 (2), 225–246.
Magnan, Avan, Dancer, Smurzynski, Probst, 1997. Reverse middle-ear transfer function in the Guinea pig measured with cubic difference tones. Hear. Res. 107 (1–2), 41–45.
Magnan, Dancer, Probst, Smurzynski, Avan, 1999. Intracochlear acoustic pressure measurements: transfer functions of the middle ear and cochlear mechanics. Audiol. Neuro. Otol. 4 (3–4), 123–128.
Middlebrooks, Bierer, 2002. Auditory cortical images of cochlear-implant stimuli: coding of stimulus channel and current level. J. Neurophysiol. 87 (1), 493–507.
Miller, 2001. Effects of chronic stimulation on auditory nerve survival in ototoxically deafened animals. Hear. Res. 151 (1–2), 1–14.
Miller, Abbas, Robinson, 1993. Characterization of wave I of the electrically evoked auditory brainstem response in the Guinea pig. Hear. Res. 69 (1–2), 35–44.
Miller, Abbas, Rubinstein, Robinson, Matsuoka, Woodworth, 1998. Electrically evoked compound action potentials of Guinea pig and cat: responses to monopolar, monophasic stimulation. Hear. Res. 119 (1–2), 142–154.
Miller, Woodruff, Pfingst, 1995. Functional responses from Guinea pigs with cochlear implants. I. Electrophysiological and psychophysical measures. Hear. Res. 92 (1–2), 85–99.
Moreno, Rajguru, Matic, Izzo, Yerram, Robinson, Hwang, et al., 2011. Infrared neural stimulation: beam path in the Guinea pig cochlea. Hear. Res. 282 (1–2), 289–302.
Palmer, Williams, 1974. Optical properties of water in the near infrared*. J. Opt. Soc. Am. 64 (8), 1107.
Rajguru, Matic, Izzo, Robinson, Fishman, Moreno, Bradley, et al., 2010. Optical cochlear implants: evaluation of surgical approach and laser parameters in cats. Hear. Res. 269 (1–2), 102–111.
Rettenmaier, Lenarz, Reuter, 2014. Nanosecond laser pulse stimulation of spiral ganglion neurons and model cells. Biomed. Opt. Express 5 (4), 1014.
Richardson, Thompson, Wise, Needham, 2017. Challenges for the application of optical stimulation in the cochlea for the study and treatment of hearing loss. Expet Opin. Biol. Ther. 17 (2), 213–223.
Richter, Matic, Izzo, Wells, Jansen, Walsh, 2011a. Neural stimulation with optical radiation. Laser Photon. Rev. 5 (1), 68–80.
Richter, Rajguru, Matic, Izzo, Moreno, Fishman, Robinson, et al., 2011b. Spread of cochlear excitation during stimulation with pulsed infrared radiation: inferior colliculus measurements. J. Neural. Eng. 8 (5), 056006.
Sato, Baumhoff, Kral, 2016. Cochlear implant stimulation of a hearing ear generates separate electrophonic and electroneural responses. J. Neurosci.: Off. J. Soc. Neurosci. 36 (1), 54–64.

Schultz, Baumhoff, Kallweit, Sato, Krüger, Ripken, et al., 2014. Optical stimulation of the hearing and deaf cochlea under thermal and stress confinement condition. SPIE BioS 8928, 1–7.
Schultz, Baumhoff, Maier, Teudt, Krüger, Lenarz, Kral, 2012. Nanosecond laser pulse stimulation of the inner ear-a wavelength study. Biomed. Opt. Express 3 (12), 3332–3345.
Snyder, Bierer, Middlebrooks, 2004. Topographic spread of inferior colliculus activation in response to acoustic and intracochlear electric stimulation. J. Assoc. Res. Otolaryngol.: JARO 5 (3), 305–322.
Snyder, Middlebrooks, Bonham, 2008. Cochlear implant electrode configuration effects on activation threshold and tonotopic selectivity. Hear. Res. 235 (1–2), 23–38.
Syka, Popelář, Kvasnák, Astl, 2000. Response properties of neurons in the central nucleus and external and dorsal cortices of the inferior colliculus in Guinea pig. Exp. Brain Res. Experimentelle Hirnforschung. Expérimentation cérébrale 133 (2), 254–266.
Tan, Rajguru, Young, Xia, Stock, Xiao, Richter, 2015. Radiant energy required for infrared neural stimulation. Sci. Rep. 5 (1), 13273.
Teudt, Maier, Richter, Kral, 2011. Acoustic events and “optophonic” cochlear responses induced by pulsed near-infrared laser. IEEE Trans. Biomed. Eng. 58 (6), 1648–1655.
Thompson, Fallon, Wise, Wade, Shepherd, Stoddart, 2015. Infrared neural stimulation fails to evoke neural activity in the deaf Guinea pig cochlea. Hear. Res. 324, 46–53.
Thompson, Wade, Brown, Stoddart, 2012. Modeling of light absorption in tissue during infrared neural stimulation. J. Biomed. Optic. 17 (7), 075002.
Tian, Wang, Wei, Lu, Xu, Xia, 2017. Short-wavelength infrared laser activates the auditory neurons: comparing the effect of 980 vs. 810 nm wavelength. Laser Med. Sci. 32 (2), 357–362.
Tozburun, Lagoda, Burnett, Fried, 2012. Subsurface near-infrared laser stimulation of the periprostatic cavernous nerves. J. Biophot. 5 (10), 793–800.
Verma, Guex, Hancock, Durakovic, McKay, Slama, et al., 2014. Auditory responses to electric and infrared neural stimulation of the rat cochlear nucleus. Hear. Res. 310, 69–75. February.
Viberg, Canlon, 2004. The guide to plotting a cochleogram. Hear. Res. 197 (1–2), 1–10.
Wells, Kao, Konrad, Milner, Kim, Mahavaden-Jansen, Jansen, 2007a. Biophysical mechanisms of transient optical stimulation of peripheral nerve. Biophys. J. 93 (7), 2567–2580.
Wells, Thomsen, Whitaker, Jansen, Kao, Konrad, Mahavaden-Jansen, 2007b. Optically mediated nerve stimulation: identification of injury thresholds. Laser Surg. Med. 39 (6), 513–526.
Xia, Tan, Xu, Hou, Mao, Richter, 2016. Pressure in the cochlea during infrared irradiation. IEEE (Inst. Electr. Electron. Eng.) Trans. Biomed. Eng. 9294 (c), 1–1.